



ISSN: 2617-6548

URL: www.ijirss.com



Enhancing photovoltaic power forecasting using deep learning techniques by considering the realized power production period: A case study on 160 kWp rooftop PV system in Thailand

 Promphak Boonraksa¹,  Terapong Boonraksa^{2*},  Warunee Srisongkram³,  Natthawath Woranetsuttikul⁴,  Boonruang Marungsri⁵

¹Department of Mechatronics Engineering, Rajamangala University of Technology Suvarnabhumi, Nonthaburi, 11000 Thailand.

²School of Electrical Engineering, Rajamangala University of Technology Rattanakosin, Salaya, Nakhon Pathom, 73170 Thailand.

³Department of Electrical Engineering, Rajamangala University of Technology Suvarnabhumi, Nonthaburi, 11000 Thailand.

⁴Department of Electrical Engineering Technology, Faculty of Industrial Technology, Phranakhon Rajabhat University, 10220 Thailand.

⁵School of Electrical Engineering, Institute of Engineering, Suranaree University of Technology, Nakhon Ratchasima, 30000 Thailand.

Corresponding author: Terapong Boonraksa (Email: terapong.boo@rmutr.ac.th)

Abstract

This paper proposes an improved PV power forecasting model by applying a modified method to three forecasting techniques: PSO-ANN, GRU, and LSTM. The key enhancement focuses on improving prediction accuracy during nighttime periods when PV systems do not generate power, an area where traditional models often yield high error rates. Reducing these inaccuracies is vital to ensure reliable energy planning and dispatch. The case study uses one-year, minute-by-minute time series generation data from a 160 kWp PV plant in Thailand. Before the modification, LSTM outperformed other methods with an MAPE of 3.91% and an RMSE of 233.09 kW. After applying the modification, adjusting nighttime power outputs to zero, the modified LSTM model achieved improved performance, with an MAPE of 2.97% and an RMSE of 232.64 kW, outperforming the modified PSO-ANN and GRU models. The simulation results confirm that this simple yet effective adjustment significantly enhances prediction accuracy by addressing a key limitation of conventional models: inaccurate power estimates during non-generating periods. Accurate PV power forecasting is essential, particularly in the early-stage investment and operational planning of PV systems.

Keywords: DL techniques, modification model, PV power forecasting, realized power production.

DOI: 10.53894/ijirss.v8i2.6378

Funding: This study received no specific financial support.

History: Received: 5 March 2025 / **Revised:** 10 April 2025 / **Accepted:** 14 April 2025 / **Published:** 22 April 2025

Copyright: © 2025 by the authors. This article is an open access article distributed under the terms and conditions of the Creative Commons Attribution (CC BY) license (<https://creativecommons.org/licenses/by/4.0/>).

Competing Interests: The authors declare that they have no competing interests.

Authors' Contributions: All authors contributed equally to the conception and design of the study. All authors have read and agreed to the published version of the manuscript.

Transparency: The authors confirm that the manuscript is an honest, accurate, and transparent account of the study; that no vital features of the study have been omitted; and that any discrepancies from the study as planned have been explained. This study followed all ethical practices during writing.

Acknowledgments: The authors would like to thank the Rajamangala University of Technology Suvarnabhumi, the Rajamangala University of Technology Rattanakosin, Phranakhon Rajabhat University, and Suranaree University of Technology, Thailand for supporting this research.

Publisher: Innovative Research Publishing

1. Introduction

Electric power is the world's main energy source and is widely used for daily use or any business operation [1, 2]. However, the vast majority of electric power generation comes from coal-based energy sources, which have a huge environmental impact due to the increasing amount of carbon dioxide from electricity generation. The international community, therefore, holds a joint meeting to discuss carbon reduction together, of which Thailand is International Energy Agency [3]; Arango-Aramburo et al. [4]; Østergaard et al. [5] and Khotsriwong et al. [6]. As a result, the power development plan, which serves as a master plan for the nation's long-term energy supply for 15 to 20 years and marks the beginning of planning for the development of a new distributed generation system, is being prepared more quickly by the Ministry of Energy, Thailand. Developing power transmission systems and purchasing electricity from abroad creates stability and sufficiency for electricity demand. It can support the improvement of the economy, society, and quality of life of the people. It plans to increase electricity generation from renewable sources, especially solar energy, from 14% today to 31% by 2032 [7].

Installing Photovoltaic (PV) power generation systems requires operators to know electric power and output value to analyze the investment worthiness [8-11]. A photovoltaic power forecasting model was developed to address this problem, and a photovoltaic power forecast model was continuously developed with various algorithms that can be applied to predict the energy accurately [12, 13]. As an illustration of advanced computational techniques, consider several widely used methods: fuzzy logic control (FLC) for handling uncertainty and approximate reasoning, genetic algorithms (GA) for optimization based on natural selection, particle swarm optimization (PSO) for simulating social behavior in search of solutions, artificial neural networks (ANN) for modelling complex patterns and decision-making processes, and artificial bee colony algorithms (ABC), which mimic the foraging behavior of bees to solve optimization problems. Each of these techniques has been applied across various fields for tasks such as optimization, decision-making, and predictive modeling [14-19]. The use of deep learning (DL) algorithms to forecast the PV power production plants' power output has grown in popularity. Various models have been employed to assess their predictive accuracy. Several separate models have been tested and shown to be successful, including GRU, RNN, and LSTM. In addition, hybrid models, which combine the strengths of different architectures, have also been explored. The PV power production forecasting has shown considerable promise with a number of hybrid DL algorithms. CNN-GRU, CNN-LSTM, CNN-BiGRU, and CNN-BiLSTM are some of the most promising designs; they all use convolutional neural networks (CNNs') advantages in conjunction with sophisticated recurrent units to increase prediction accuracy [20-23].

Many researchers are interested in studying PV power forecasting, which can be compared with previous studies and existing works, as shown in Table 1. However, using these algorithms still gives poor predictability of the solar system's output power. The characteristics of the separate algorithms were then integrated to create a mixed prediction model, such as a neural network-based mixed prediction technique. Particle Swarm Intelligence Optimized-based Artificial Neural Network prediction greatly enhanced the prediction outcomes [24, 25]. Forecasting using DL techniques is a simple forecasting method and simple modelling, but output forecasting may be an overlooked point that is a significant error. Therefore, this paper develops a DL forecasting model to make predictions more accurate by incorporating another function. This paper used data on solar photovoltaic power generation systems in the central region of Thailand, with an installed size of 160 kWp. Accurate forecasts would benefit stakeholders in decision-making regarding investment planning for solar power plant installations.

Table 1.
Previous studies comparison.

References	Techniques	Input Data	Shot Summary	Outstanding Techniques
Seyedmahmoudian, et al. [26]	PSO, DE, and the combination of both methods known as DEPSO.	The PV irradiance (W/m^2), Ambient temperature ($^{\circ}C$), PV power output (W).	Mathematically forecasting the short-term PV output power.	DEPSO
Li, et al. [20]	CNN and LSTM.	Date hour, PV power output (W).	PV output power prediction via a hybrid deep learning approach.	Hybrid CNN and LSTM
Kuo, et al. [21]	ANN, LSTM, and GRU model.	Weather, and PV data.	Forecasting of PV power in the short term suggests a new method for analyzing sky images to determine cloud coverage.	The cloud coverage rate via the deep learning methods GRU and LSTM.
Sansine, et al. [27]	The PSO algorithm combined with XGBoost (PSO-XGBoost), the PSO combined with Gradient	Ambient temperature ($^{\circ}C$), Humidity (%), Atmospheric pressure (mbar), Wind velocity (m/s), Dew point temperature ($^{\circ}C$) and the	Solar Irradiance Forecasting.	PSO-LSTM

References	Techniques	Input Data	Shot Summary	Outstanding Techniques
	Boosting Regression (PSO-GBR), and PSO-LSTM.	wind direction, amount of rain, Solar irradiance (W/m^2), and the clear-sky model.		
Gumar and Demir [28]	ANN, PSO-ANN, ABC-ANN, and GA-ANN.	Date, Time, Humidity, Atmospheric pressure, Panel temperature, Ambient temperature, PV irradiance (W/m^2), PV power output (W).	Predicting the PV power. Develop the hybrid model with an ANN base.	PSO-ANN
Devi and Srivenkatesh [29]	Artificial Gorilla Troops Optimizer (AGTO), TLO, RNN, LSTM, KNN.	Weather data, PV power output (W).	A metaheuristic optimization algorithm was applied for the PV power forecasting.	GC-TLBO
Poti, et al. [19]	Physical approach PV power forecasting.	Irradiance (W/m^2), PV panel temperature ($^{\circ}C$), ambient temperature ($^{\circ}C$) and PV panel specification.	Forecasting of PV power generation in the short term. Examination of the correlation of PV power on summer days versus winter days.	No comparison with other methods
Khotsriwong, et al. [6]	CNN, RNN, GRU, BiGRU, LSTM, and BiLSTM. The hybrid models: CNN-GRU, CNN-BiGRU, CNN-LSTM, and CNN-BiLSTM.	Photovoltaic (PV) power output (W), solar radiation (W/m^2), PV panel temperature ($^{\circ}C$), and wind velocity (m/s) data.	Short-term photovoltaic power output prediction.	CNN-BiGRU BiLSTM
Abumohsen, et al. [30]	LSTM, GRU, and RNN.	Date (dd), hour (hr), weekday, week number, month, year, temperature ($^{\circ}C$), and energy (Wh)	Load forecasting in power system.	GRU
Miraftabzadeh, et al. [22]	The Linear, Dense, CNN, and LSTM techniques have been assessed.	Date hour, PV power output (W).	Introduces the transfer learning approach for utilizing trustworthy, trained deep learning algorithms in day-ahead PV power forecasting.	LSTM, Transferred LSTM
Our work	PSO-ANN, GRU, and LSTM techniques with modifications.	Date hour, PV irradiance (W/m^2), Ambient temperature ($^{\circ}C$), and PV power output (W).	Long-term PV power forecasting: A comparative analysis of PV power forecasting results obtained by applying prominent deep learning techniques on a real-site solar rooftop.	M-LSTM

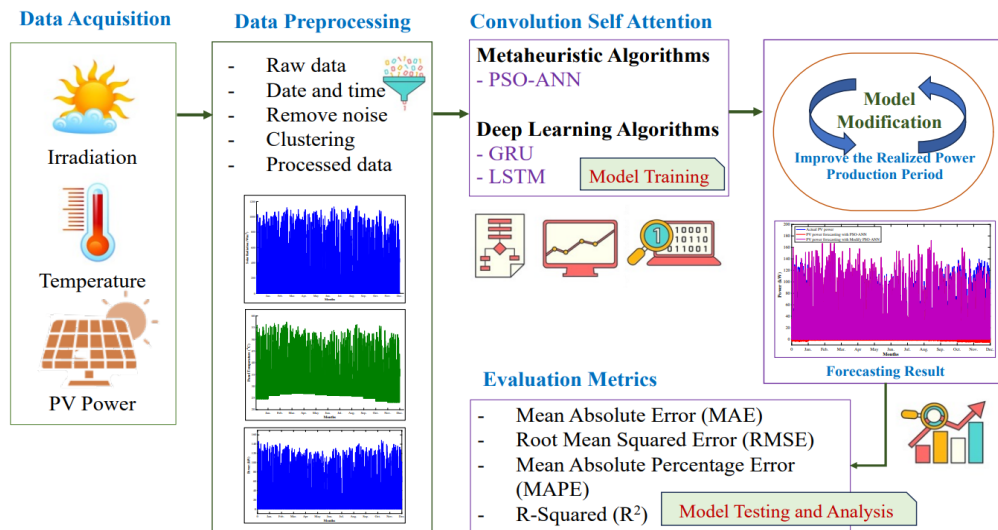


Figure 1.

A proposed framework that uses deep learning techniques to anticipate PV power and incorporates the historical power production era for improved accuracy is presented.

Figure 1 shows the proposed flow of PV power forecasting using deep learning techniques by considering the realized power production period. As a result, the main contributions of this study can be summarized as follows:

- This paper presents a comparative analysis of PV power forecasting results obtained by applying prominent deep-learning techniques on a real-site solar rooftop in Thailand. The study aims to elucidate the effectiveness and performance of these techniques in accurately forecasting PV power generation.
- The PV power forecasting techniques were compared, including PSO-ANN, GRU, and LSTM techniques. The performance of these techniques will be evaluated against actual PV power data using key indicators such as MAE, MAPE, RMSE, and R^2 .
- This paper developed a forecasting model for the PV power generation system, which involves considering the actual power production periods by incorporating the observed power generation periods.

The remaining section of the paper is organized as follows: The PV power forecasting techniques are presented in Section 2. Section 3 introduces the forecasting technique. A case study of the PV power generating system, the accuracy analysis, and the forecasting model are presented in Section 4. Section 5 presents the forecasting results and provides a detailed discussion of the model's accomplishments. Finally, Section 6 summarizes the key findings of the study, highlighting the most successful models and offering suggestions for future work or improvements in PV power forecasting methodologies.

2. The PV Power Forecasting Methods

Various techniques, including statistical, machine learning, heuristic, and physical approaches, may be used to predict the electricity output of solar systems. These techniques are based on two main approaches to modeling PV power forecasting. One approach is physical, which requires knowledge of photovoltaic material properties, system metadata, and the information requirements of climate conditions. A second approach is a data-driven approach that requires operational data on the PV system to train the forecasting model. A data-driven approach can be applied after the PV system is installed and running, and there is sufficient data to train/calibrate the model. The drawback of the physical model is that it requires too many input variables. Heuristic models are introduced to minimize the number of input variables required in PV power forecasting. Because these models rely on the relationship between climatic data, including solar irradiance, temperature, and PV power production, they are categorized as data-driven models. By reducing input complexity, these models aim to maintain or even enhance prediction accuracy while improving computational efficiency. Several heuristic models have been developed on similar principles for forecasting the PV power from irradiation and module temperature, but they differ only in optimal model parameters. Heuristic models have the main advantage that parameters can be obtained from historical data of PV power generation systems with ease. To predict PV output power generation, statistical methods and machine learning techniques are often employed, utilizing historical data on PV power production. Both of these approaches are data-driven, meaning they depend heavily on the availability, quality, and accuracy of operational data to build reliable forecast models. By analyzing past performance and identifying patterns within the data, these methods enable more accurate predictions of future PV power output, providing valuable insights for energy management and grid stability. Usually, the more historical data available, the better the PV forecasting model can be trained in operating behavior under different climatic conditions, and hence the better the forecast accuracy [25, 31, 32]. While the physical technique requires a physical parameter as input, the data-driven approach, depicted in Figure 2, requires historical data to train.

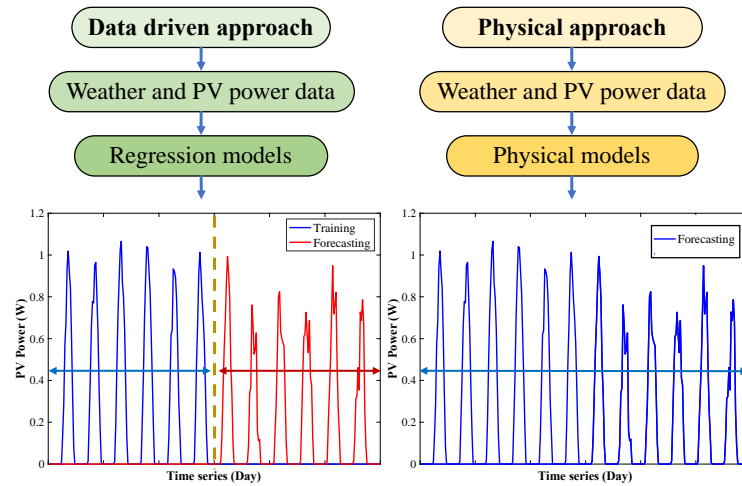


Figure 2. Schematic of the data-driven and the physical approaches for PV power forecasting.

3. The Forecasting Techniques

3.1. Artificial Neural Networks

The ANNs are made up of several non-linear arithmetic units, or neurons, and their connections. Thus, a neural network is a computer system that works similarly to the biological neural network of the human brain. It manages large amounts of data and learns from input to produce results. Neural networks are widely used for prediction tasks because they analyze input parameters and identify the optimal relationship between input and output variables. By learning from data, neural networks can effectively map complex relationships that may not be easily captured by traditional techniques. Neural networks can be applied in various fields, including machine learning, image processing, computer science, optimization, forecasting, etc. An ANN typically consists of three layers: the input layer, which is the one that receives the data first; the hidden layer, which is responsible for processing data after it has been received; and the output layer, which gets data that has been processed by the hidden layer. An ANN consists of three main layers: the input layer (receiving raw data), the next part is the hidden layer (processing data), and the output layer (generating results). A neural network model was developed using MATLAB's nftools to forecast photovoltaic power generation [33]. Figure 3 shows the ANN model developed using the nftools application in the MATLAB program.

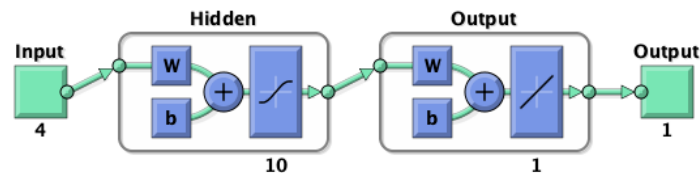


Figure 3. The ANN model via nftools in MATLAB.

3.2. Particle Swarm Optimization Algorithms

The PSO is modeled after the cooperative behavior of bird flocks, where members cooperate to accomplish a shared objective, including locating food or avoiding predators. This approach was first developed in 1995 by Eberhart and Kennedy, who aimed to model the social behavior and cooperation seen in nature to solve optimization problems. It is an evolutionary computational technique that is easy to use and has simple parameters. In PSO algorithms, a solution is given to particles that can move in the search direction. Each particle has a best solution linked with it, called pbest; moreover, the PSO monitors the global best value, termed gbest. The PSO method updates the particle's location and velocity continually until it reaches the objective function's optimal value [33]. A random velocity and position are assigned for each swarm in the PSO algorithm, with each swarm having its fitness value at each iteration. A comparison and update will be performed between the global best (gbest) and the personal best group (pbest). The swarm velocity and position are updated at each iteration using Equations 1 and 2, where these two vectors are required for the precise determination of each particle's position [25, 34].

$$V_{(k+1)} = wV_{(k)} + c_1r_1(p_{best(k)} - X_{(k)}) + c_2r_2(g_{best(k)} - X_{(k)}) \tag{1}$$

$$X_{(k+1)} = X_{(k)} + V_{(k+1)} \tag{2}$$

Where r_1 and r_2 are numbers that were randomly generated and have a value between 0 and 1, c_1 and c_2 are constant values of acceleration, and w is the particle's inertia weight.

3.3. Long Short-Term Memory Model

This section provides a brief overview of the LSTM algorithm. The LSTM was selected due to its widespread popularity and strong efficiency in previous studies. Despite having the same goal, various deep learning algorithms have different

mathematical models, strengths, and disadvantages. The LSTM was designed to tackle the long-term dependency issue in traditional RNNs. The memory unit in an LSTM network takes the role of an RNN's hidden layer neurons. An input gate, a forget gate, and an output gate are the three main components that comprise the memory unit's construction. These gates enable the network to selectively delete erroneous data or store important information at each time step, effectively managing the flow of information and enhancing learning over long sequences. Capable of learning temporal relationships of recurrent networks, LSTM has emerged as one of the most suitable networks in various domains. This timing relationship is typical in photovoltaic power generation because it depends on solar intensity and environmental conditions and is difficult to understand and forecast [30, 35, 36]. Figure 4 shows the structure of an LSTM block diagram. The fundamental concept behind LSTM is its memory cell, which can retain information over extended periods. This memory cell consists of an internal state (referred to as the cell state vector) that can be updated by adding new information or forgetting outdated information.

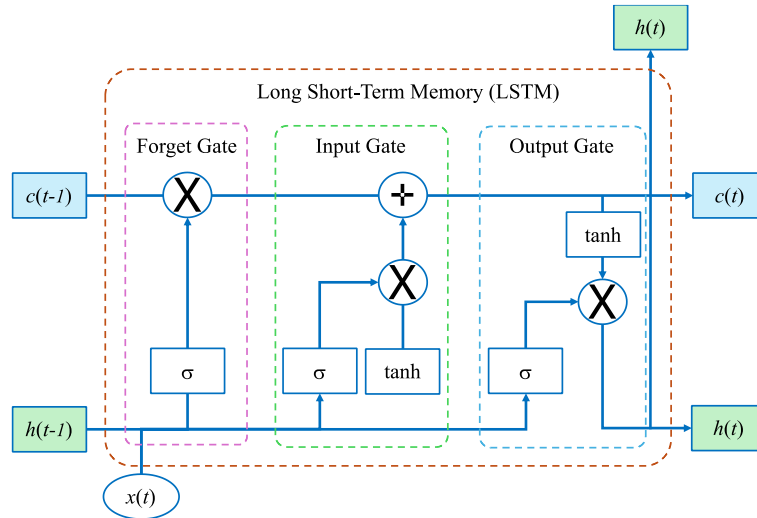


Figure 4.
A block diagram structure of the LSTM.

In LSTM networks, the three primary gates that regulate information flow are the Forget, Input, and Output gates. To avoid needless memory retention, the Forget Gate analyzes the previous cell state and decides which data should be deleted. The input gate controls the flow of fresh information into the cell memory to ensure that relevant information is stored for processing later. Lastly, the Output Gate controls which data from the cell memory is sent to the following layer, which affects the network's ultimate output. These gates collectively enable LSTM networks to efficiently manage long-term dependencies in sequential data processing. These gates work together to ensure that relevant information is retained while irrelevant data is removed, enhancing the network's ability to learn from long sequences effectively. Both gates utilize a sigmoid activation function followed by pointwise multiplication to regulate the information flow. The Output Gate controls the information that will be output from the memory cell. Together, these gates ensure that the LSTM can effectively manage long-range dependencies, allowing it to learn and retain patterns over time. Equation 3 illustrates how the gates work by combining the output from the previous time step, the cell state vector, and the current input.

$$f_t = \sigma(W_f \cdot [h_{t-1}, x_t] + b_f) \tag{3}$$

In this case, f_t is the Forget Gate's activation vector, which decides which data from the prior cell state should be deleted; W_f is the weight matrix associated with the input; x_t is the input vector in the present time step for the LSTM unit; b_f is the bias term added to the input, and h_{t-1} is the preceding time step's hidden condition vector, which influences the current decision-making process of the gate. The Input Gate determines which fresh data from the current input should be included after the Forget Gate has filtered the prior cell state. This process is regulated by the sigmoid function, ensuring that only relevant data is incorporated into the cell state. By selectively updating its memory, the LSTM model enhances its ability to retain important information while discarding less significant data, improving sequential data processing. Thus, the activation vector for the input/update gate can be expressed by Equation 4. This cycle uses an input modulation gate to manage the new value. The input modulation gate equation is similar to the input gate equation but utilizes a \tanh function, shown in Equation 5.

$$i_t = \sigma(W_i \cdot [h_{t-1}, x_t] + b_i) \tag{4}$$

$$C_t^* = \tanh(W_C \cdot [h_{t-1}, x_t] + b_C) \tag{5}$$

The cell state vector C_t updates the memory by combining two components: the old memory, which passes through the forget gate, and the new memory, which passes through the input gate, expressed by Equation 6.

$$C_t = f_t \times C_{t-1} + i_t \times C_t^* \tag{6}$$

The output gate decides which information to retrieve from the memory, depending on specific conditions. The activation vector o_t of the output gate can be specified as described in Equation 7. The LSTM unit h_t output vector derived from C_t is subsequently processed by the \tanh function, as shown in Equation 8.

$$o_t = \sigma(W_o \cdot [h_{t-1}, x_t] + b_o) \tag{7}$$

$$h_t = o_t \times \tanh(C_t) \tag{8}$$

3.4. Gate Recurrent Unit Model

The GRU is a gating mechanism for RNNs introduced in 2014. Like LSTM networks, GRUs also incorporate gating mechanisms, but with a simpler architecture. The Update Gate and the Reset Gate are the only two gates in GRU, as opposed to the Forget Gate and Output Gate found in LSTM. This design reduces the number of parameters, making GRU more computationally efficient. This absence of an output gate can give GRU an edge in certain tasks, especially when working with smaller or less frequent datasets, where overfitting may be a concern. GRU can be seen as an improvement on the hidden layer of traditional RNNs, as it enables better handling of long-term dependencies by adaptively updating and resetting hidden states. Its schematic and structural layout is depicted in Figure 5. showing how these gates function together to update the network’s memory and control information flow [30, 37].

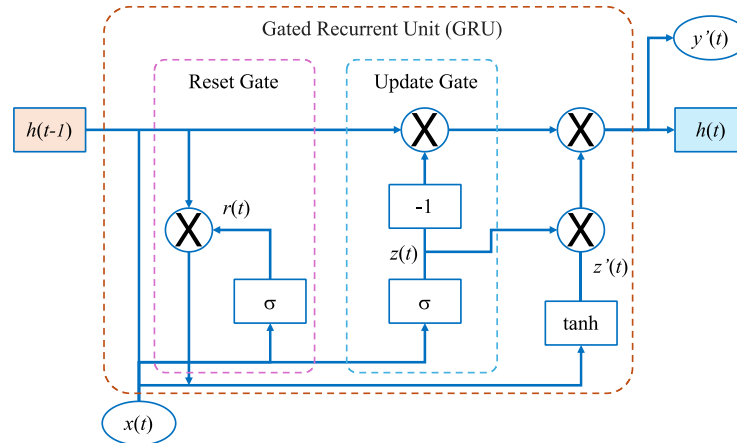


Figure 5.
The ANN model via nftools in MATLAB.

The pertinent symbols are as follows:

- At time step t , the input to the network is represented by the variable $x(t)$.
- The data vectors $h(t)$ and x correspond to the temporal output and the immediate hidden layer output at time t , respectively.
- The gate vectors $z(t)$ and $r(t)$ are defined such that $z(t)$ is the update gate, $r(t)$ is the reset gate output at time step t .
- The network utilizes two activation functions: the sigmoid function, denoted as $\sigma(x)$, and the tanh function, denoted as $\tanh(x)$.

The GRU model operates similarly to the LSTM model, beginning with the GRU receiving the current input and the previous hidden state. These two components are processed through the reset gate, which determines how much of the previous memory should be forgotten before updating the current state. This mechanism enables the model to effectively control the flow of information while retaining relevant context in sequential data. Overall, GRU offers a simpler structure compared to LSTM while still maintaining the ability to manage information flow and context efficiently [35, 38]. The reset gate vector is mathematically defined in Equation 9. Moreover, the update gate controls which values are to be stored or added, as described in Equation 10.

$$z_t = \sigma(W_z \cdot [h_{t-1}, x_t] + b_z) \tag{9}$$

$$r_t = \sigma(W_r \cdot [h_{t-1}, x_t] + b_r) \tag{10}$$

Once the reset gate has been passed through, the candidate activation vector h_t is calculated as illustrated in Equation 11. In the GRU model, the candidate activation primarily influences updates to the hidden state. Based on the previous hidden state and the current input, it represents the potential change to the hidden state. This mechanism allows the GRU to efficiently capture relevant information and discard unnecessary details, thereby improving its ability to model sequential data. As a result, the GRU model's final output is derived from Equation 12, which combines the candidate activation with the update gate to produce the updated hidden state.

$$h\tilde{t} = \tanh(W_h \cdot [r_t \cdot h_{t-1}, x_t] + b_c) \tag{11}$$

$$h_t = (1 - z_t) * h_{t-1} + z_t * h\tilde{t} \tag{12}$$

4. Research Methodology

4.1. PV Power Generation System a Case Study

Forecasting the PV output power requires the model’s input data for training. For this research, the five-input data was selected: date, hour, solar intensity, solar panel temperature, ambient temperature, and PV power for one year. This data is obtained from the solar power plant in the central region of Thailand, collecting data in 2023. The annual solar intensity data

for the case study area is presented in Figure 6. Additionally, Figure 7 shows the monthly solar intensity data for January 2023, providing a more detailed view of solar radiation patterns during that specific month.

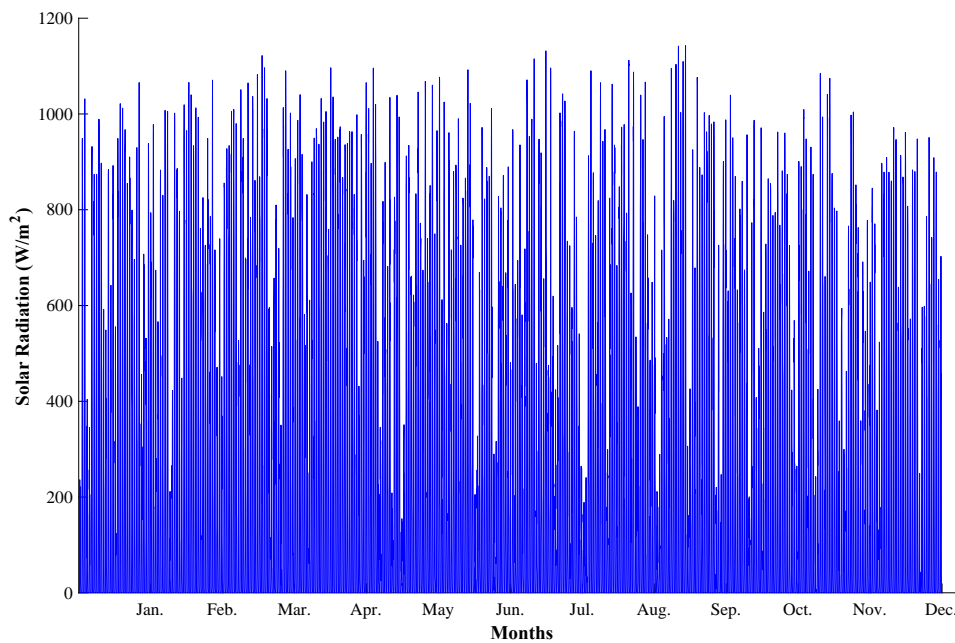


Figure 6.
The annual PV irradiation of the case study location.

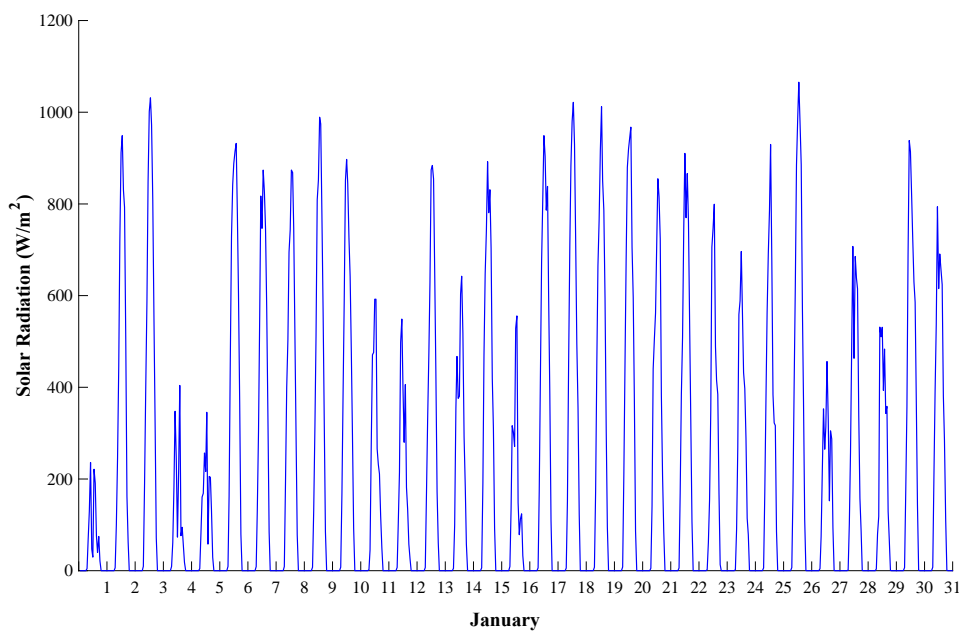


Figure 7.
Monthly solar radiation in January.

The annual solar panel temperature data was used for a case study, as shown in Figure 8. The highest temperature is 57 degrees Celsius in February. Figure 9 shows the case study area's annual photovoltaic power generation system output.

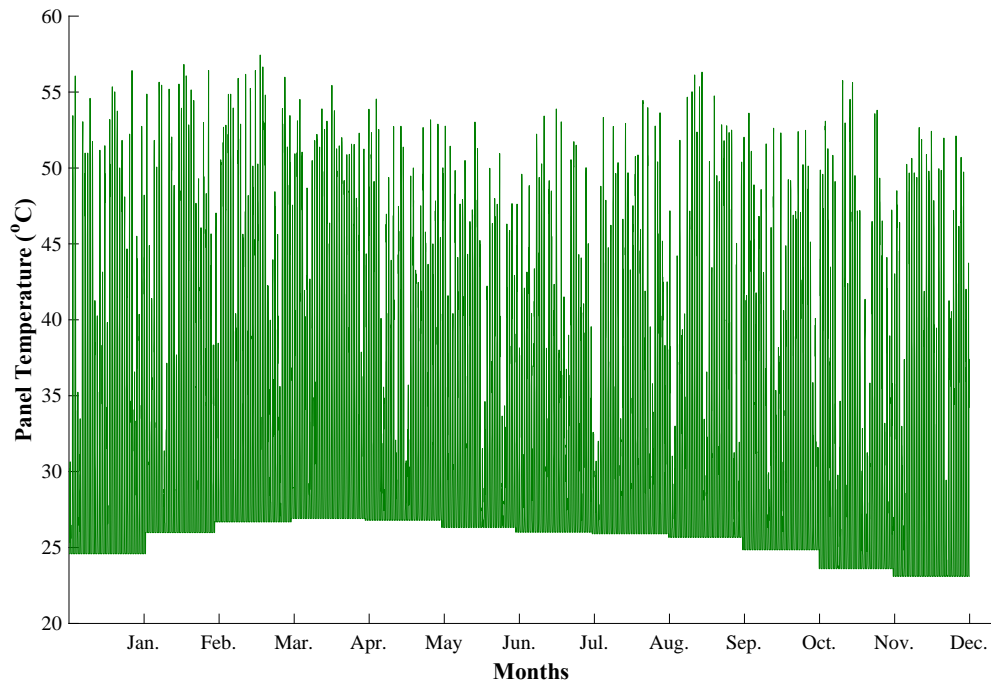


Figure 8.
The annual solar panel temperature of the case study area.

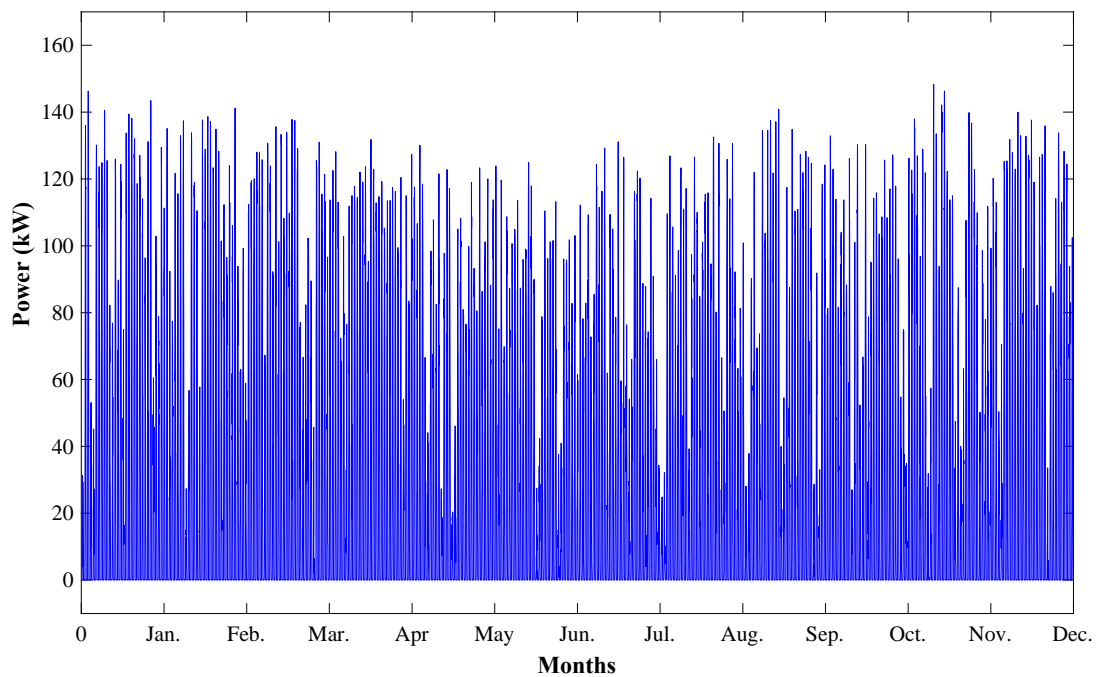


Figure 9.
The annual PV power generation system output power of the case study area.

4.2. The PV Power Forecasting with PSO-ANN Technique

The PSO-ANN hybrid prediction model combines the PSO method with an ANN to create an enhanced predictive system. In this approach, PSO optimizes the weights and parameters of the ANN to improve its learning capabilities and accuracy. The ANN is designed to mimic the structure and function of the human nervous system, utilizing repetitive learning to identify patterns and correlations based on previous data. By learning from repeated experiences, the ANN can improve its ability to predict outcomes. Figure 10 depicts the structure of the neural model, which is modeled after the human nervous system, acting as a training network that adjusts itself to better achieve target outcomes.

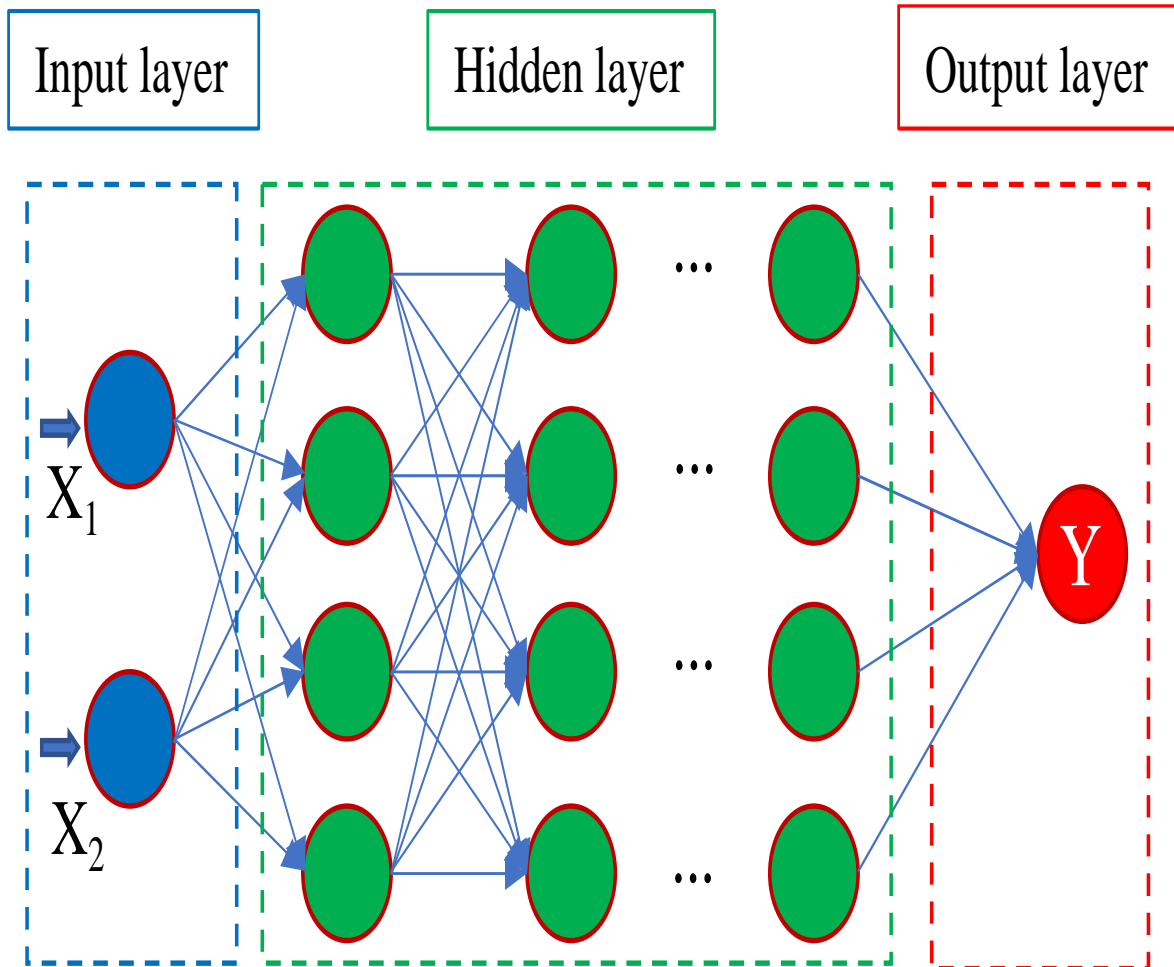


Figure 10.
The functional structure of the neural network.

This model makes use of a multilayer feed-forward neural network, more precisely a backpropagation network, which is renowned for its intricacy and extremely non-linear structure. In this type of network, each neuron is associated with a weight that is initially assigned randomly. The PSO enhances this process by optimizing the network's parameters, which leads to more efficient learning and improved prediction accuracy. By effectively adjusting the weights through the PSO algorithm, the model can converge more quickly to an optimal solution, resulting in better performance in tasks such as classification and regression. These weights influence the strength of connections between neurons and are adjusted during the learning process. In order to determine the best output for every neuron, the network also makes use of a variety of activation or transfer functions, including Tan-sigmoid, Log-sigmoid, and Linear functions. Three main layers make up the neural network architecture: the input layer accepts data, the hidden layer processes it, and the output layer provides the final classification or prediction. The network's backpropagation algorithm allows it to learn by minimizing error through the adjustment of weights, iterating over the dataset until the output aligns with the desired target [24, 39]. The first step in creating the hybrid power forecasting model with the PSO-ANN method was to identify how many particles would be used in the structure of the ANN algorithm.

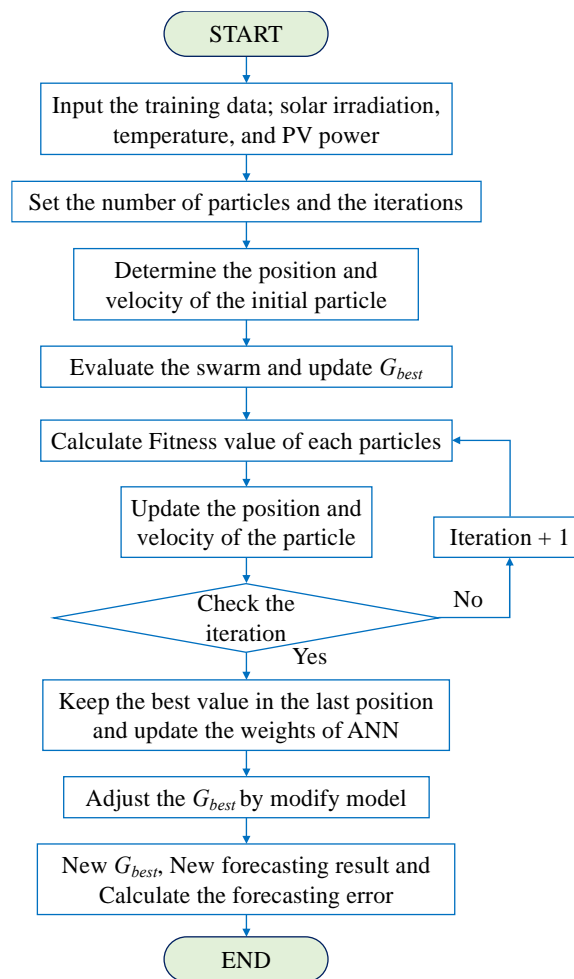


Figure 11.
Block diagram of the M-PSO-ANN power forecasting model.

The process begins by sampling the particles, which involves specifying their weight, position, and velocity. Next, the neural network is simulated, and the suitability of the initial particles is assessed. Following this, the best global best (g_{best}) and personal best (p_{best}) values are identified, and the suitability of each particle within the neural network structure is calculated. The best fitness value in the group is determined during each iteration, leading to improvements in particle velocity and position. This procedure is continued until the maximum iterations is achieved after the ideal values for the current set of particles are gathered. Figure 11 shows the functional diagram of the MPSO-ANN power forecasting model. After the simulations were completed, the researchers noticed that much power was generated during the night. Therefore, a command model was created to adjust the power generated at night to zero.

4.3. The PV Power Forecasting with DL Techniques

This section outlines the detailed steps and configurations used to implement the DL technique. The technique is developed and executed using the Keras library within a Jupyter notebook, utilizing Python as the programming language. The training and testing processes are conducted on a machine powered by an Intel(R) Core(TM) i7-8750H CPU that operates at 2.20 GHz. Performance is optimized and training time is decreased with this configuration, which guarantees effective management of the computational load throughout the deep learning model training phase. The hardware and software configurations, including GPU usage, memory allocation, and batch sizes, are carefully adjusted to balance speed and accuracy. The detailed setup parameters used for the training process are outlined in Table 2, providing a clear overview of the environment in which the models are trained. Since the outcomes of all models ranged from 9 to 12 epochs, the training method for all DL models used an epoch number of 10. The learning rate for each model was dynamically adjusted using the Adam optimizer, an adaptive learning rate optimization algorithm. By altering the learning rate according to the first and second moments of the gradients, this method improves convergence speed and overall performance. By employing the Adam optimizer, the models achieve more efficient training, allowing them to better capture complex patterns in the data. Figure 12 shows the steps involved in implementing the proposed DL approach for PV power forecasting. The process begins with the initialization of the weight parameters for each generation. The PV system's input data is then read and processed. The deep learning models are then trained on the dataset, iterating until they converge to an optimal solution. Finally, the trained models are evaluated using a test dataset, and performance is measured through accuracy metrics to determine the effectiveness of each technique.

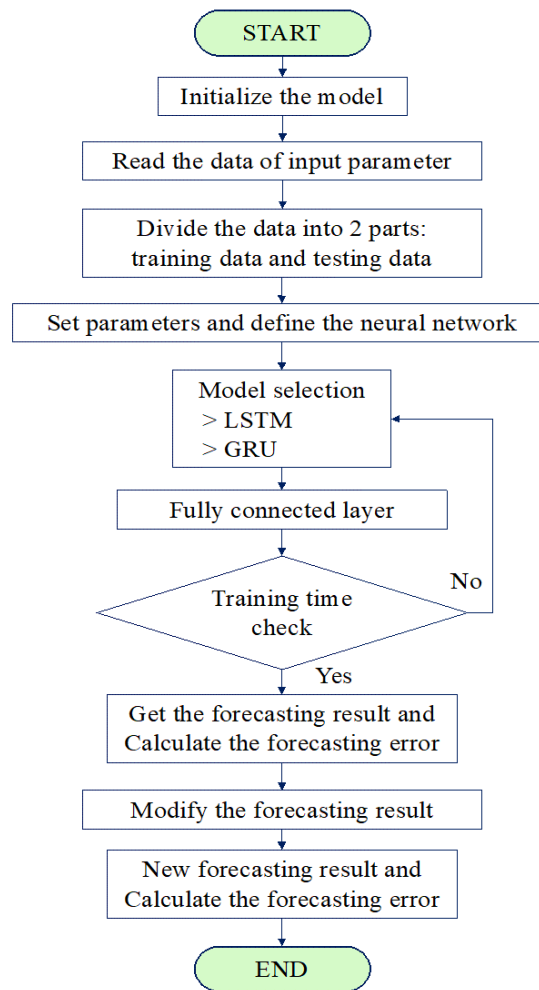


Figure 12. Flow chart of DL models application on PV power forecasting.

Table 2. Parameters Setting for Deep Learning Techniques.

Models	Parameters	Values
GRU and LSTM	Number of FC-layer	3 (50, 100, 100)
	Number of neural layers	2 (1, 256)
	Activation function	<i>sigmoid</i>
	Dropout	0.1
	Optimizer	Adam
	Loss	MAE

4.4. Accuracy Analysis

Forecast accuracy is important since it shows how closely the actual values match the model’s forecasts. A model is considered highly accurate and reliable if its forecast results deviate minimally from the real outcomes. Several methods are employed to evaluate the accuracy of PV forecasting, which is crucial for optimizing the integration of solar energy into power systems. Accurate forecasting helps utilities manage supply and demand effectively, ensuring grid stability and reducing operational costs. Among the various metrics used to assess the accuracy of forecasting models, the Mean Absolute Error (MAE) and Mean Absolute Percentage Error (MAPE) are two of the most commonly employed. One of the popular metrics for evaluating the precision of forecasting models is the Root Mean Squared Error (RMSE), especially in domains like energy management, finance, and meteorology. An accurate measure of the model’s performance is provided by RMSE, which computes the square root of the average squared discrepancies between the observed and predicted values. This metric is very useful since it can be used to measure the degree of prediction error, which gives information on the efficacy and dependability of the model [40, 41]. This article mentions the coefficient of determination (R^2) as one of its metrics. This statistical metric shows how much of the variance in the dependent variable in a regression model can be explained by the independent variable. It gives insight into the model’s quality of fit. In this article, five performance indicators are introduced: MAE, MAPE, Percent Error, RMSE, and R^2 . The MAE is defined as the average of the absolute variances between anticipated and actual values, which provides a simple measure of accuracy. Both the MAE and MAPE can be calculated using Equations 13 and 14, offering a way to evaluate the model’s predictive performance by comparing it against actual PV power output.

The Error and RMSE can be calculated from Equations 15 and 16. The R^2 has a value ranging from 0 to 1. A value of $R^2 = 1$ indicates that the model explains all the variability in the dependent variable, signifying a perfect fit, while an $R^2 = 0$ suggests that the model does not explain any variability, indicating a poor fit. So, the higher value of R^2 means the more accurate the model [42]. The R^2 can be calculated from Equation 17.

$$MAE = \frac{1}{n} \sum_{i=1}^n |y_i - \hat{y}_i| \tag{13}$$

$$MAPE(\%) = \frac{1}{n} \sum_{i=1}^n \left| \frac{y_i - \hat{y}_i}{\hat{y}_i} \right| \times 100 \tag{14}$$

$$ERROR(\%) = \left| \frac{y_i - \hat{y}_i}{\hat{y}_i} \right| \times 100 \tag{15}$$

$$RMSE = \sqrt{\frac{1}{n} \sum_{i=1}^n (y_i - \hat{y}_i)^2} \tag{16}$$

$$R^2 = 1 - \frac{\sum_{i=1}^n (y_i - \hat{y}_i)^2}{\sum_{i=1}^n (y_i - \bar{y}_i)^2} \tag{17}$$

Where y_i and \hat{y}_i are the PV power forecasting and the real PV power output at time i^{th} , \bar{y}_i is the mean of PV power output, respectively. The number of forecasting time series is denoted by n .

5. Results and Discussion

The PV power forecasting results of the PV system were forecasted using MATLAB with the input parameters, as shown in section IV, and to assess the prediction findings' accuracy, a number of metrics were employed. Forecasting using PSO-ANN, LSTM, and GRU techniques uses 1,000 calculation cycles. The PV forecasting results using the PSO-ANN as shown in Figure 13; annual simulation results show large discrepancies, especially at night. Therefore, the researchers improved the forecasting results for nighttime forecasts to zero to make the model more accurate. Figures 14 and 15 show the annual simulation results using the LSTM and GRU techniques, respectively, both of which produce similar outcomes. When compared to the PSO-ANN simulation results, it is evident that the LSTM and GRU techniques have fewer errors, particularly during nighttime conditions, where the PSO-ANN technique exhibits higher error rates.

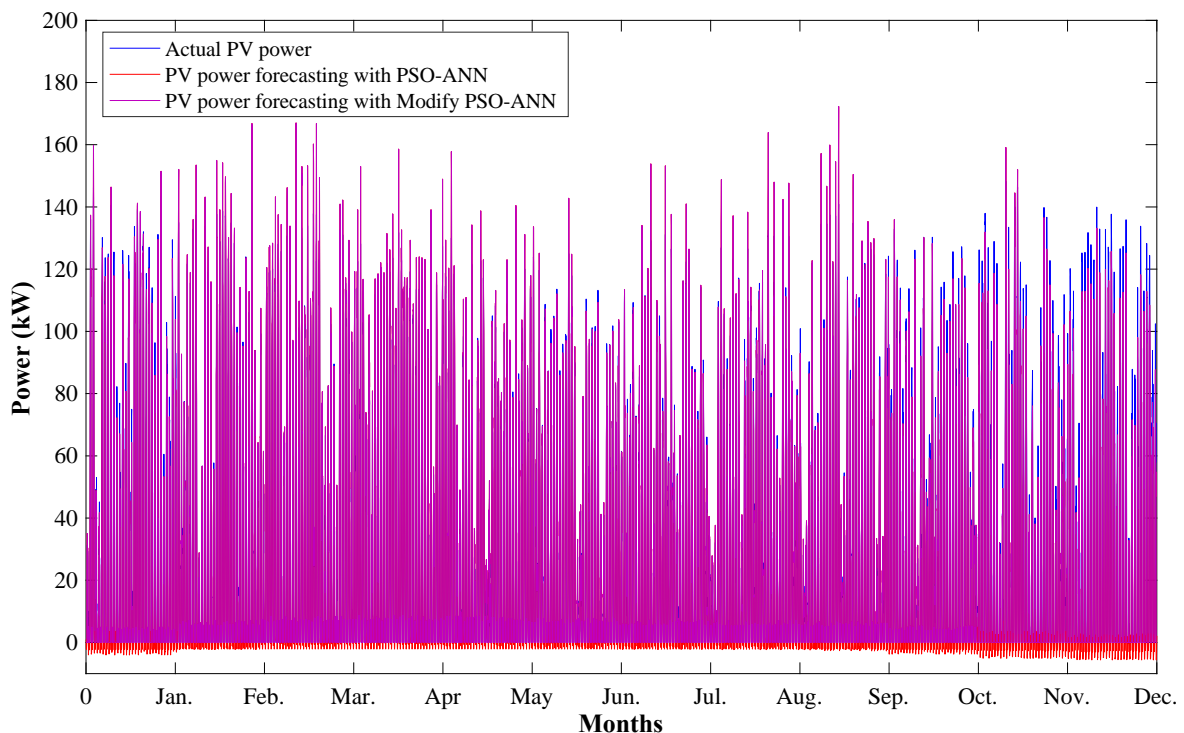


Figure 13 Annual PV power forecasting using the PSO-ANN technique.

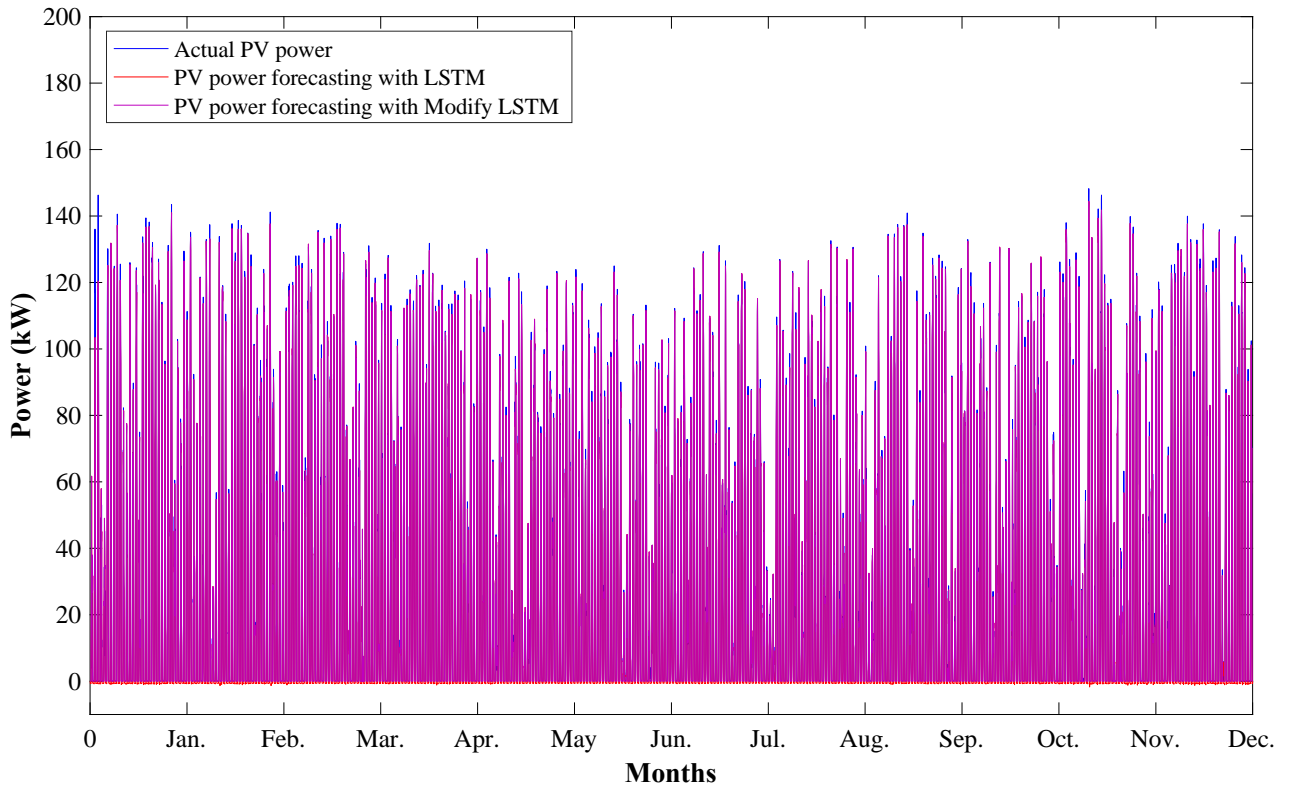


Figure 14.
Annual PV power forecasting using the LSTM technique.

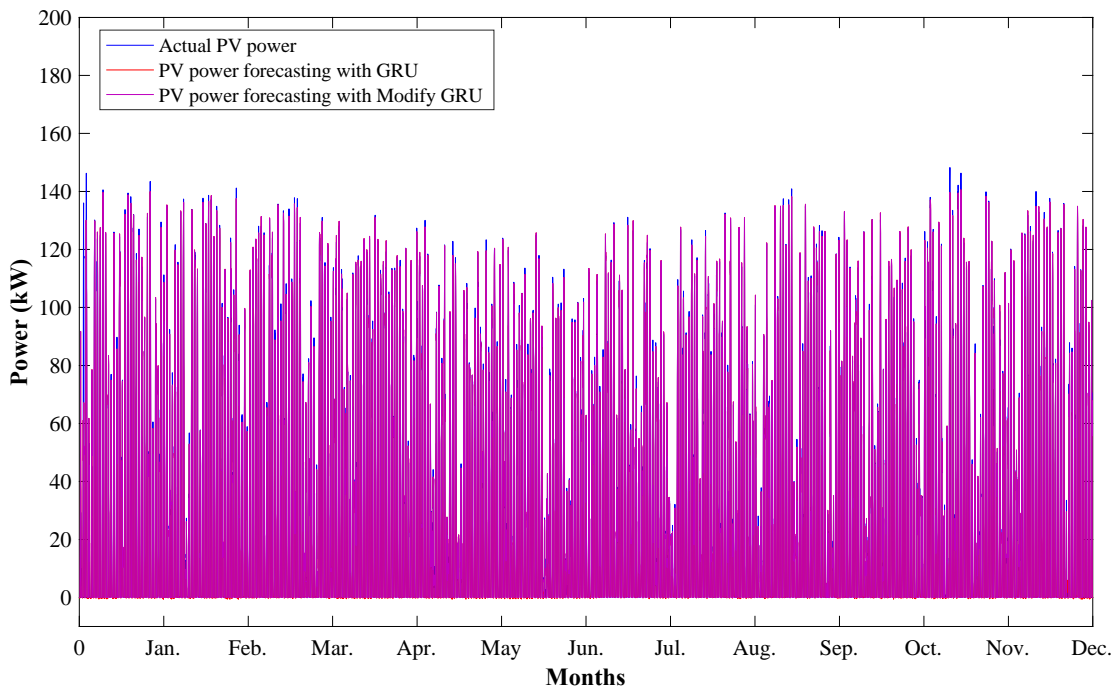


Figure 15.
Annual PV power forecasting using the GRU technique.

Figure 16 shows the PV power output comparison of three forecasting techniques without modification, which shows the seven-day forecast from December 25-31. The daily simulation results using PSO-ANN, LSTM, and GRU techniques are displayed in Figures 17 to 19, respectively. These results demonstrate that the system does not generate any power after the model is modified in the middle period from the graph, and that the prediction results from the LSTM and GRU techniques are the ones that are closest to the real PV power generation. However, the forecast results still show quite a discrepancy during the night. The output power prediction results of the solar power generating system employing the PSO-ANN, GRU, and LSTM methods are shown in Figures 20-22. The linear regression analysis reveals that the GRU and LSTM procedures are more accurate than the PSO-ANN techniques. The forecasting results converge towards the Linear line, which has regression values of 0.997 and 0.998, respectively.

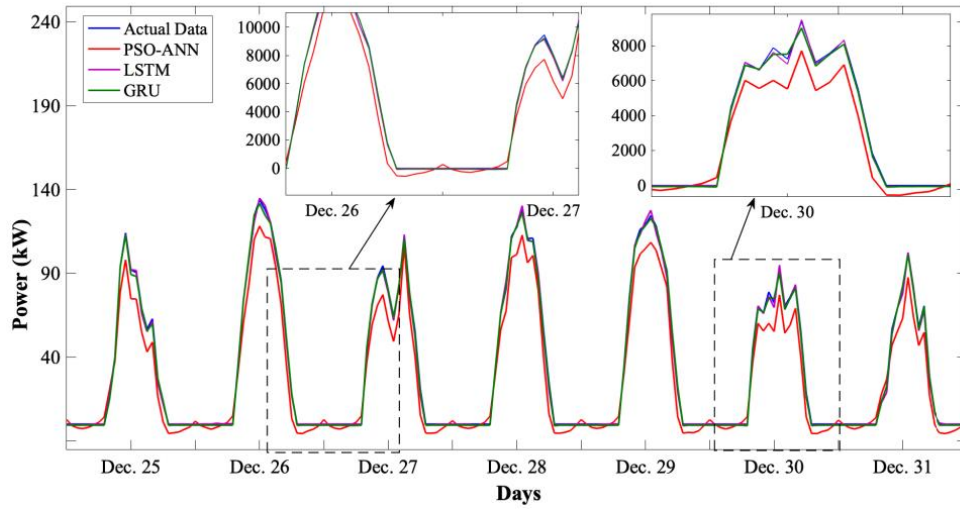


Figure 16
The PV power output comparison of three forecasting techniques without modification.

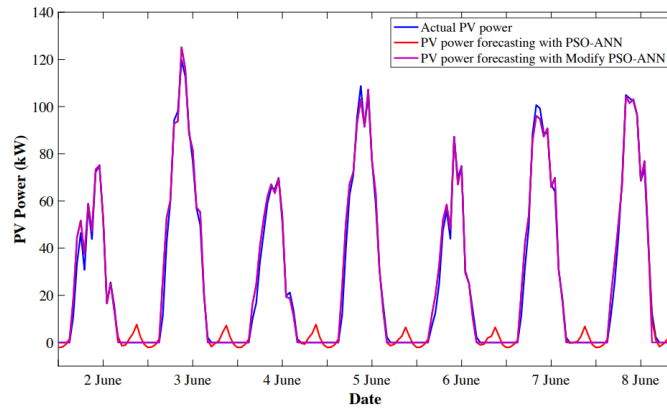


Figure 17.
Weekly PV power forecasting using the PSO-ANN technique.

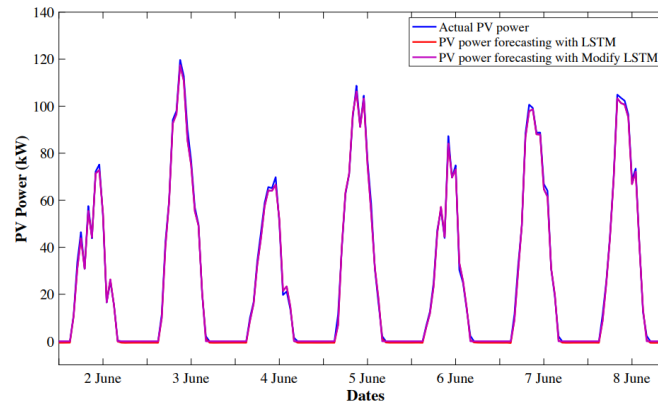


Figure 18.
Weekly PV power forecasting using the LSTM technique.

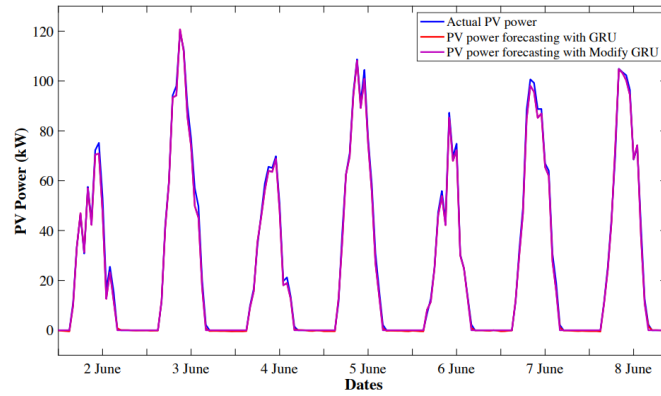
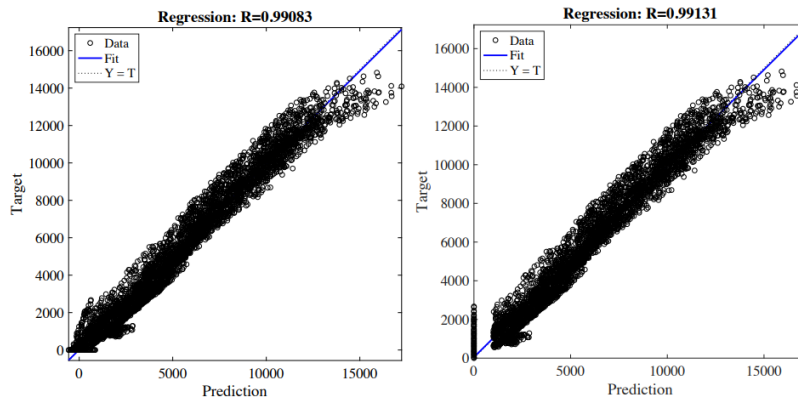
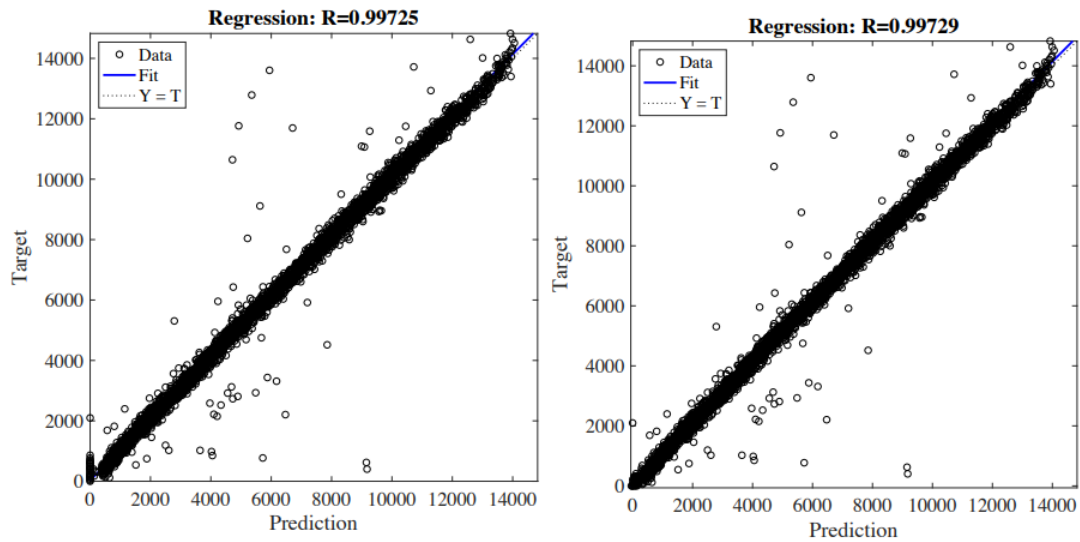


Figure 19.
Weekly PV power forecasting using the GRU technique.



a) PSO-ANN technique b) Modify PSO-ANN technique

Figure 20.
Linear regression of the PV power forecasting results using the PSO-ANN technique.



a) GRU technique b) Modify GRU technique

Figure 21.
Linear regression of the PV power forecasting results using the GRU technique.

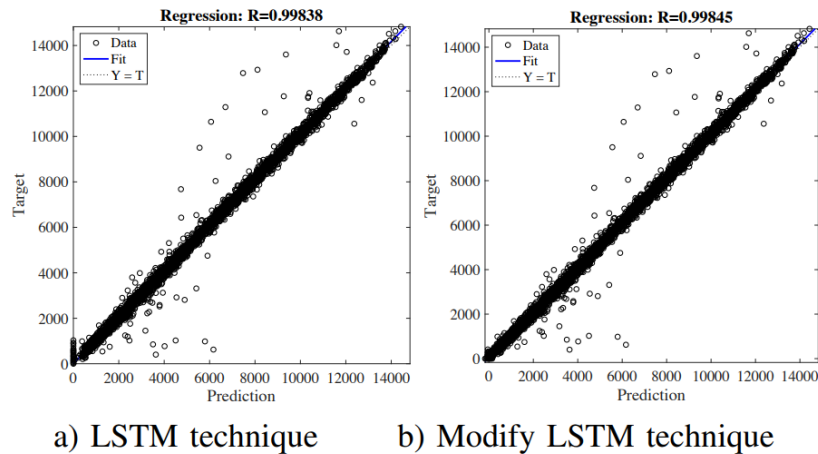


Figure 22. Linear regression of the PV power forecasting results using the LSTM technique.

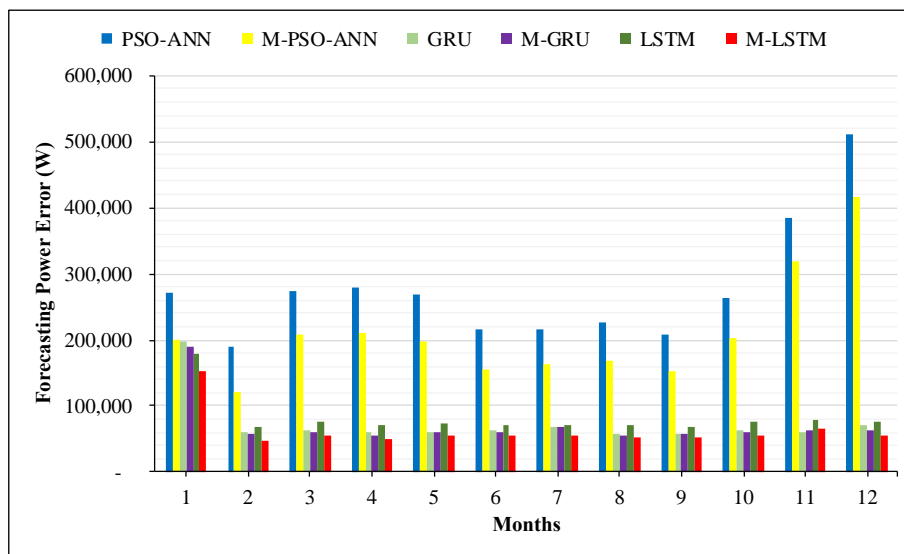


Figure 23. The forecasting power error for each month.

Table 3. Comparison of PV output power forecasting results.

Techniques	Without Modifying Techniques			Modify Techniques		
	MAE (kW)	MAPE (%)	RMSE (kW)	MAE (kW)	MAPE (%)	RMSE (kW)
PSO-ANN	378.45	13.18	532.15	287.04	9.99	519.69
GRU	100.75	3.50	297.69	97.71	3.40	295.04
LSTM	112.36	3.91	233.09	85.30	2.97	232.64

To illustrate the precision of the suggested methods, Table 3 presents a comparison of PV power forecasting. When comparing the forecasting results using the MAE metric across three models, the GRU technique initially demonstrated the highest accuracy with an MAE of 112.36 kW. However, after modifications to the model, the LSTM technique outperformed the others, achieving an MAE of 85.30 kW, making it the most accurate model. Comparing the simulation results with the model’s MAPE indicators shows that the GRU technique has the highest accuracy, with a MAPE value of 3.50%. However, after model improvements, the LSTM technique becomes the most accurate, achieving an MAPE value of 2.97%. A comparison of the simulation results using the MAPE indicators confirms that the LSTM technique outperforms other methods, with an initial RMSE of 233.09 kW. Following the model improvements, the RMSE is further reduced to 232.64 kW, reinforcing its accuracy in power prediction. The LSTM approach offers the lowest predicting error, according to the PV output power forecasting findings. This demonstrates that the LSTM approach outperforms the PSO ANN and GRU approaches in terms of accuracy. The fact that power is created while the system is not producing power is the weakness of the three deep learning approaches. Because it is a random value, if such a technique is to be used, the input values must be adjusted before entering the model, or the output values must be adjusted after the forecasting is made, for the results to be accurate and as expected. The simulation findings indicate that using the M-LSTM model to set nighttime power to zero enhances forecast results and lowers simulation result error levels. Figure 23 presents the error values for the monthly PV

forecasting. The results indicate that the LSTM technique consistently exhibits the lowest error values. Notably, the M-LSTM technique stands out among the other methods, demonstrating superior accuracy in power prediction.

6. Conclusion

PV power generation systems are increasingly being installed nowadays, making pre-installation planning crucial. This planning involves forecasting both the power produced and the potential profit of the PV system. Accurate forecasting requires comprehensive data from previous power generation systems for model training. Traditionally, PV power forecasting has faced challenges, particularly during nighttime operations when solar energy production is absent or significantly reduced. Predictions during these periods have often been inaccurate due to the randomness of nighttime conditions. Despite this, some electrical energy can still be generated, albeit minimally, which complicates prediction accuracy. This study focuses on improving PV power forecasting accuracy, particularly during nighttime, by employing advanced deep learning techniques. We compared the performance of different techniques and enhanced them to better account for PV power generation. This paper applies the approach involving training data sets that include 24-hour energy production records encompassing day and night cycles. By incorporating nighttime data into the training process, the aim is to mitigate the errors in power predictions during these periods. Specifically, the effectiveness of the M-LSTM technique is evaluated compared to other methods, such as PSO-ANN and GRU techniques. The simulation results demonstrate that the M-LSTM technique exhibits superior accuracy when compared against the other approaches. This work advances the accuracy of PV power forecasts by utilizing deep learning algorithms and optimizing them for nighttime settings. For PV power production systems to operate as efficiently and profitably as possible, planning and operation must be optimized, and this requires greater forecasting capabilities.

References

- [1] B. Alves, "Global electricity consumption 1980-2018," Technical report," Retrieved: <https://hal.archives-ouvertes.fr/docs/00/36/68/58/PDF/ale2d.pdf>. [Accessed September 1, 2024], 2018.
- [2] D. Jones, "Global electricity review 2021," Technical report," Retrieved: <http://www.emberclimate.org/globalelectricityrevig12021>. [Accessed September 1, 2024], 2021.
- [3] International Energy Agency, "Global energy review 2021 assessing the effects of economic recoveries on global energy demand and CO2 emissions in 2021," Technical report," Retrieved: <https://www.iea.org/reports/global-energy-review-2021>. [Accessed September 1, 2024], 2021.
- [4] S. Arango-Aramburo, S. Bernal-García, and E. R. Larsen, "Renewable energy sources and the cycles in deregulated electricity markets," *Energy*, vol. 223, p. 120058, 2021. <https://doi.org/10.1016/j.energy.2021.120058>
- [5] P. A. Østergaard, R. M. Johannsen, and N. Duic, "Sustainable development using renewable energy systems," *International Journal of Sustainable Energy Planning and Management*, vol. 29, pp. 1-6, 2020. <https://doi.org/10.5278/ijsep.2020.29.1>
- [6] N. Khotsriwong, P. Boonraksa, W. Sarapan, T. Boonraksa, N. Boonrakchat, and B. Marungsri, "Short-term load demand forecasting using supervised deep learning techniques: A case study of suranaree university of technology," presented at the 2023 International Electrical Engineering Congress (iEECON), September 2–6, ; Krabi, Thailand, 2023.
- [7] Energy Policy and Planning Office, *Thailand power development plan 2015–2036 (PDP2015)*. Thailand: Ministry of Energy, 2021.
- [8] J. Antonanzas, N. Osorio, R. Escobar, R. Urraca, F. J. Martínez-de-Pison, and F. Antonanzas-Torres, "Review of photovoltaic power forecasting," *Solar Energy*, vol. 136, pp. 78–111, 2016. <https://doi.org/10.1016/j.solener.2016.06.069>
- [9] M. Florio, *The evaluation framework: A cost-benefit analysis model*. Cambridge, MA, United States: MIT Press Direct, 2019.
- [10] Z. Mustafa, R. Iqbal, M. Siraj, and I. Hussain, "Cost benefit analysis of suranaree university of technology in agriculture sector of Quetta," *Environmental Sciences Proceedings*, vol. 23, no. 1, p. 26, 2022. <https://doi.org/10.3390/envirosci2022023026>
- [11] S. B. K. Ntsaluba and I. Dlamini, "Performance and cost analysis for a university based solar PV installation," presented at the 2020 IEEE PES/IAS Power Africa, Nairobi, Kenya, 2020.
- [12] M. Rana, I. Koprinska, and V. G. Agelidis, "Univariate and multivariate methods for very short-term solar photovoltaic power forecasting," *Energy Conversion and Management*, vol. 121, pp. 380-390, 2016. <https://doi.org/10.1016/j.enconman.2016.05.025>
- [13] K. J. Iheanetu, "Solar photovoltaic power forecasting: A review," *Sustainability*, vol. 14, no. 24, p. 17005, 2022. <https://doi.org/10.3390/su142417005>
- [14] Y. Tao and Y. Chen, "Distributed PV power forecasting using genetic algorithm based neural network approach," in *Proceedings of the 2014 International Conference on Advanced Mechatronic Systems, Aug. 2014; Kumamoto, Japan*, 2014, pp. 557-560.
- [15] Z. P. Ncane and A. K. Saha, "Forecasting solar power generation using Fuzzy Logic and artificial neural network," presented at the 2019 Southern African Universities Power Engineering Conference/Robotics and Mechatronics/Pattern Recognition Association of South Africa (SAUPEC/Rob-Mech/PRASA). 28-30 Jan. 2019; Bloemfontein, South Africa, 2019.
- [16] J. Hao, X. Sun, and Q. Feng, "A novel ensemble approach for the forecasting of energy demand based on the artificial bee colony algorithm," *Energies*, vol. 13, no. 3, p. 550, 2020. <https://doi.org/10.3390/en13030550>
- [17] P. R. Kumari, P. Bojja, B. Pragathi, T. Prasanth Kumar Reddy, and P. Vijaya Lakshmi, "Evaluation and implementation of particle swarm optimization Maximum power point tracking technique for photo voltaic system," *Journal of Physics: Conference Series*, vol. 1804, no. 1, p. 012188, 2021.
- [18] Y. Zhou *et al.*, "Short-term solar power forecasting based on convolutional neural network and analytical knowledge," *International Transactions on Electrical Energy Systems*, vol. 31, no. 11, p. e13111, 2021. <https://doi.org/10.1002/2050-7038.13111>
- [19] K. D. Poti, R. M. Naidoo, N. T. Mbungu, and R. C. Bansal, "Intelligent solar photovoltaic power forecasting," *Energy Reports*, vol. 9, pp. 343-352, 2023. <https://doi.org/10.1016/j.egyr.2023.09.004>
- [20] G. Li, S. Xie, B. Wang, J. Xin, Y. Li, and S. Du, "Photovoltaic power forecasting with a hybrid deep learning approach," *IEEE Access*, vol. 8, pp. 175871–175880, 2020. <https://doi.org/10.1109/ACCESS.2020.3025612>

- [21] W.-C. Kuo, C.-H. Chen, S.-Y. Chen, and C.-C. Wang, "Deep learning neural networks for short-term PV Power Forecasting via Sky Image method," *Energies*, vol. 15, no. 13, p. 4779, 2022. <https://doi.org/10.3390/en15134779>
- [22] S. M. Miraftebadeh, C. G. Colombo, M. Longo, and F. Foiadelli, "A day-ahead photovoltaic power prediction via transfer learning and deep neural networks," *Forecasting*, vol. 5, no. 1, pp. 213-228, 2023. <https://doi.org/10.3390/forecast5040013>
- [23] N. Khortsriwong, P. Boonraksa, and T. Boonraksa, "Performance of deep learning techniques for forecasting PV power generation: A case study on a 1.5 MWp Floating PV power plant," *Energies*, vol. 16, no. 15, p. 2119, 2023. <https://doi.org/10.3390/en16052119>
- [24] A. Nespoli, E. Oglari, and S. Leva, "Day-ahead photovoltaic forecasting: A comparison of the most effective techniques," *Energies*, vol. 12, no. 9, p. 1621, 2019. <https://doi.org/10.3390/en12091621>
- [25] P. Dawan, K. Sriprapha, and S. Kittisontirak, "Comparison of power output forecasting on the photovoltaic system using adaptive neurofuzzy inference systems and particle swarm optimization artificial neural network model," *Energies*, vol. 13, no. 2, p. 351, 2020. <https://doi.org/10.3390/en13020351>
- [26] M. Seyedmahmoudian *et al.*, "Short-term forecasting of the output power of a building-integrated photovoltaic system using a metaheuristic approach," *Energies*, vol. 11, no. 5, p. 1260, 2018. <https://doi.org/10.3390/en11051260>
- [27] V. Sansine, P. Ortega, D. Hissel, and M. Hopuare, "Solar irradiance probabilistic forecasting using machine learning, metaheuristic models and numerical weather predictions," *Sustainability*, vol. 14, no. 22, p. 15260, 2022. <https://doi.org/10.3390/su142315260>
- [28] A. K. Kumar and F. Demir, "Solar photovoltaic power estimation using meta-optimized neural networks," *Energies*, vol. 15, no. 22, p. 8669, 2022. <https://doi.org/10.3390/en15238669>
- [29] K. Devi and M. Srivenkatesh, "An advanced hybrid meta-heuristic model for solar power generation forecasting via ensemble deep learning," *Ingénierie des Systèmes d'Information*, vol. 28, no. 5, pp. 1395-1407, 2023. <https://doi.org/10.18280/isi.280528>
- [30] M. Abumohsen, A. Y. Owda, and M. Owda, "Electrical load forecasting using LSTM, GRU, and RNN algorithms," *Energies*, vol. 16, no. 5, p. 2283, 2023. <https://doi.org/10.3390/en16152283>
- [31] P. Gupta and R. Singh, "PV power forecasting based on data-driven models: A review," *International Journal of Sustainable Engineering*, vol. 14, no. 6, pp. 1733-1755, 2021. <https://doi.org/10.1080/19397038.2021.1986590>
- [32] I. Kaaya and J. Ascencio-Vasquez, "Photovoltaic power forecasting methods," *Solar Radiation - measurement, modeling and forecasting techniques for photovoltaic solar energy applications*, *IntechOpen*, p. 97049, 2022. <https://doi.org/10.5772/intechopen.105682>
- [33] M. T. Ansari and M. Rizwan, "Ann and PSO based approach for solar energy forecasting: A step towards sustainable power generation," in *Proceedings of the 2021 4th International Conference on Recent Developments in Control, Automation and Power Engineering (RDCAPE)*. 7-8; Noida, India, 2021, pp. 413-417.
- [34] N. Y. Dahlan, S. Zamri, M. I. A. Zaidi, A. M. Azmi, and R. Zailani, "Forecasting generation of 50mw gambang large scale solar photovoltaic plant using ann-psy," *International Journal of Renewable Energy Research*, vol. 12, no. 1, pp. 10-18, 2022. <https://doi.org/10.35833/ijrer.2022.12282>
- [35] W.-C. Kuo, C.-H. Chen, S.-H. Hua, and C.-C. Wang, "Assessment of different deep learning methods of power generation forecasting for solar PV system," *Applied Sciences*, vol. 12, no. 15, p. 7529, 2022. <https://doi.org/10.3390/app12147529>
- [36] J. Yu *et al.*, "Deep learning models for PV power forecasting," *Energies*, vol. 17, no. 16, p. 3973, 2024. <https://doi.org/10.3390/en17163973>
- [37] R. Asghar, F. R. Fulginei, M. Quercio, and A. Mahrouch, "Artificial neural networks for photovoltaic power forecasting: A review of five promising models," *IEEE Access*, vol. 12, pp. 90461-90485, 2024. <https://doi.org/10.1109/access.2024.3420693>
- [38] J. Chen, X. Huang, H. Jiang, and X. Miao, "Low-cost and device-free human activity recognition based on hierarchical learning model," *Sensors*, vol. 21, no. 7, p. 2359, 2021. <https://doi.org/10.3390/s21072359>
- [39] A. El Kounni, H. Radoin, H. Mastouri, H. Bahi, and A. Outzourhit, "Solar power output forecasting using artificial neural network," in *Proceedings of the 2021 9th International Renewable and Sustainable Energy Conference (IRSEC)*, 23-27 Nov. 2021, Morocco, 2021, pp. 1-7.
- [40] H. Swalehe, P. Boonraksa, and T. Boonraksa, "Short-term forecasting model for photovoltaic generation systems using adaptive neuro-fuzzy inference system," in *Proceedings of The Eighth National Symposium and the Fourth International Symposium, Bangkokthonburi University, April 26; Thailandp*, 2020, pp. 51-57.
- [41] N. H. A. Rahman, M. Z. Hussin, S. I. Sulaiman, M. A. Hairuddin, and E. H. M. Saat, "Univariate and multivariate short-term solar power forecasting of 25MWac Pasir Gudang utility-scale photovoltaic system using LSTM approach," *Energy Reports*, vol. 9, pp. 387-393, 2023. <https://doi.org/10.1016/j.egy.2023.09.018>
- [42] A. A. Lateko, H.-T. Yang, and C.-M. Huang, "Short-term PV power forecasting using a regression-based ensemble method," *Energies*, vol. 15, no. 11, p. 4171, 2022.